ISBN: 978-3-95450-222-6 ISSN: 2673-5350 doi:10.18429/JACoW-IBIC2020-WEPP22

# SUBMICROPULSE ENERGY-TIME CORRELATIONS OF 40-MeV ELECTRON BEAMS AT FAST*

R. Thurman-Keup†, A. H. Lumpkin, Fermi National Accelerator Laboratory, Batavia, IL, USA


*Abstract*

We have recently extended our ability to explore submicropulse effects in relativistic electron beams to energy-time (E-t) correlations. The Fermilab Accelerator Science and Technology (FAST) facility consists of a photoinjector, two superconducting TESLA-type capture cavities, one superconducting ILC-style cryomodule, and a small ring for studying non-linear, integrable beam optics called IOTA. The linac contains, as part of its instrumentation, an optical transport system that directs optical transition radiation (OTR) from an Al-coated Si surface to an externally located streak camera for bunch length measurements. For the first time, an OTR screen after the spectrometer magnet was used for measurements of submicropulse E-t correlations. The projected, micropulse time profile was fit to a single Gaussian peak with $\sigma = 11.5 \pm 0.5$ ps for 500 pC/micropulse and with a 200-micropulse synchronous sum, in agreement with the upstream bunch-length measurement at a non-energy-dispersive location. The submicropulse E-t images were explored for four rf phases of CC1, and the E vs. t effects will be presented.


## INTRODUCTION

The Fermilab Accelerator Science and Technology (FAST) facility was constructed for advanced accelerator research [1]. It consists of a photoinjector-based electron linac followed by an ILC-type cryomodule and a small ring called IOTA (Integrable Optics Test Accelerator) for studying non-linear optics among other things [2]. Presently under construction, is an RFQ-based proton injector to supply protons to the IOTA ring. To support operations in the electron linac, an optical transport system was installed to take light from various sources (synchrotron radiation, transition radiation) and send it to various instruments including a Hamamatsu streak camera located outside the enclosure [3]. In this paper, we present the first measurements from a newly installed optical transport line that takes optical transition radiation (OTR) from an Al-coated Si surface after the spectrometer magnet to the streak camera. The transport is arranged in such a way as to map the energy direction of the OTR screen to the spatial direction in the streak camera, allowing for a measurement of the energy-time (E vs. t) phase space of a micropulse.

## FAST FACILITY

The FAST facility (Fig. 1) begins with a 1.3 GHz normal-conducting rf photocathode gun with a $Cs_2Te$-coated cathode. The photoelectrons are generated by irradiation with a YLF laser at 263 nm that can provide several μJ per pulse [4]. Following the gun are two superconducting 1.3 GHz capture cavities (CC1 and CC2) that accelerate the beam to its design energy of around 50 MeV. After acceleration, there is a section for doing round-to-flat beam transforms, followed by a magnetic bunch compressor and a short section that can accommodate small beam experiments. At the end of the experimental section is a spectrometer dipole which can direct the beam to the low energy dump. If the beam is not sent to the dump, it enters the ILC-type cryomodule where it receives up to 250 MeV of additional energy and is sent to either a high-energy dump or the IOTA ring. Table 1 lists the typical beam parameters.

Table 1: Beam Parameters for FAST

| Parameter | Value |
|---|---|
| Energy | 20 – 300 MeV |
| Micropulse Charge | < 10 fC – 3.2 nC |
| Micropulse Frequency | 0.5 – 9 MHz |
| Macropulse Duration | ≤ 1 ms |
| Macropulse Frequency | 1 – 5 Hz |
| Transverse Emittance | > 1 µm |
| Micropulse Length | 0.9 – 70 ps |

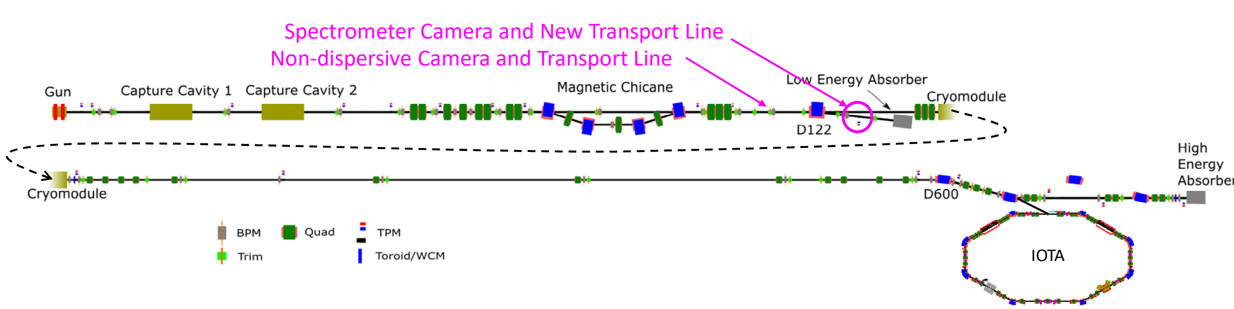


Figure 1: Layout of the FAST facility. D122 is the spectrometer magnet, after which is the OTR source for the new optical transport line.

* This manuscript has been authored by Fermi Research Alliance, LLC under Contract No. DE-AC02-07CH11359 with the U.S. Department of Energy, Office of Science, Office of High Energy Physics.
† keup@fnal.gov

Content from this work may be used under the terms of the CC BY 3.0 licence (© 2020). Any distribution of this work must maintain attribution to the author(s), title of the work, publisher, and DOI

ISBN: 978-3-95450-222-6 ISSN: 2673-5350 doi:10.18429/JACoW-IBIC2020-WEPP22

## EXPERIMENTAL SETUP

The experimental setup used for these measurements utilizes a new transport line for the existing Optical and Terahertz Instrumentation System, OTIS [3] (see Fig. 2).

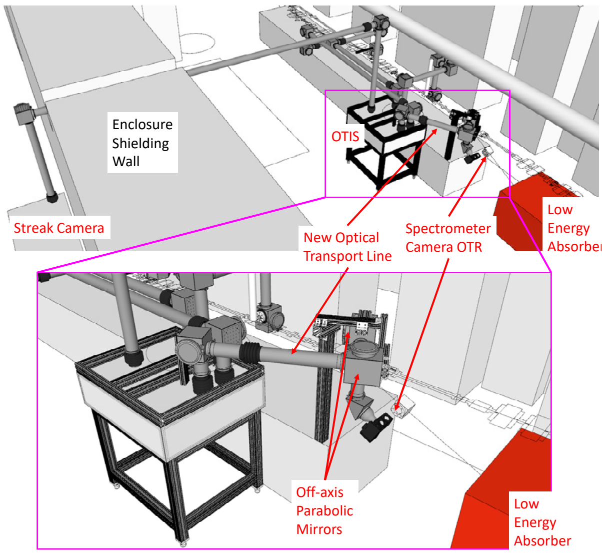


Figure 2: Overview the Optical and Terahertz Instrumentation System (OTIS). The new transport line originates from the spectrometer camera.

The new transport line originates at the optical transport for the spectrometer camera (Fig. 3) where it splits the OTR light coming from the Al-coated Si plate using a Thorlabs BP245B1 pellicle-type beamsplitter and sends half the light through a pair of Edmund Optics 35-564 off-axis paraboloidal mirrors to collimate the light before transport to the Hamamatsu C5680 streak camera. The streak camera is equipped with mirror input optics to reduce optical dispersion, and a M5675 synchroscan unit to

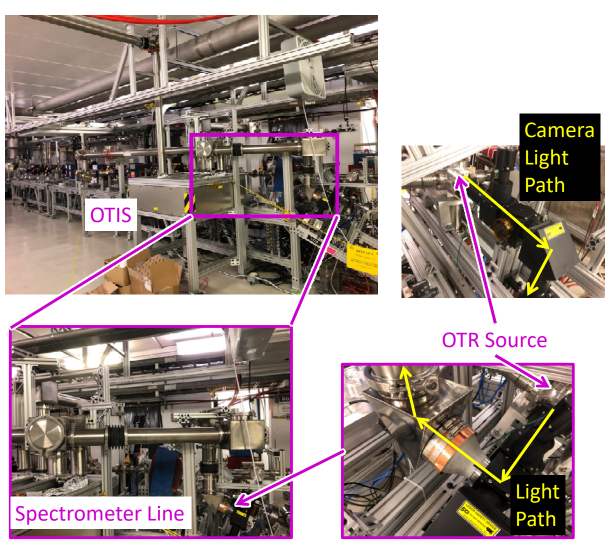


Figure 3: Pictures showing the new optical transport line from the spectrometer camera source point. The yellow arrows show the beginning light path for the new transport line and the spectrometer camera.

enable the accumulation of many micropulses while avoiding significant phase jitter (see [5] for more details). The transport line itself is comprised of stainless steel (SS316) boxes with flat mirrors, and 4-inch-diameter SS316 tubes.

Figure 4 shows the effective optical path for the light originating from the OTR screen. From the OTR source, the light propagates through a focusing section before encountering the beam splitter. At that point, the light to the streak camera traverses two off-axis paraboloidal mirrors to collimate the light which travels ~14 meters to the streak camera.

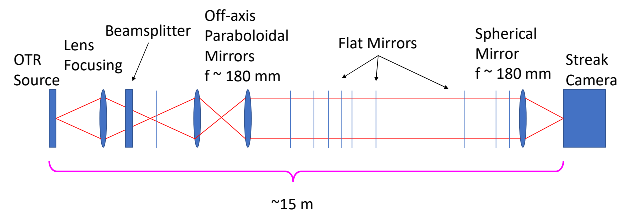


Figure 4: Effective optical path of the new transport line from OTR source, to streak camera (not to scale). There are 10 flat mirrors (indicated by the thin lines) in addition to the labeled optical components.

The alignment of the transport line was accomplished via a laser injected through a viewport on the input side of the spectrometer magnet. It was focused at the location of the OTR screen and allowed to exit by reflection off the screen which allowed us to both align and adjust the collimation of the transport line (Fig. 5). In attempting to align the transport line it was discovered that the OTR screen is not positioned at 45 degrees to the beam. It appears to be off by about 5 degrees which complicated the alignment slightly as the focusing properties of off-axis parabolic mirrors are sensitive to the position and direction of the light. In Fig. 5, the misalignment can be seen at the beamsplitter. This caused the light to follow a zig-zag path inducing distortion from the paraboloidal mirrors.

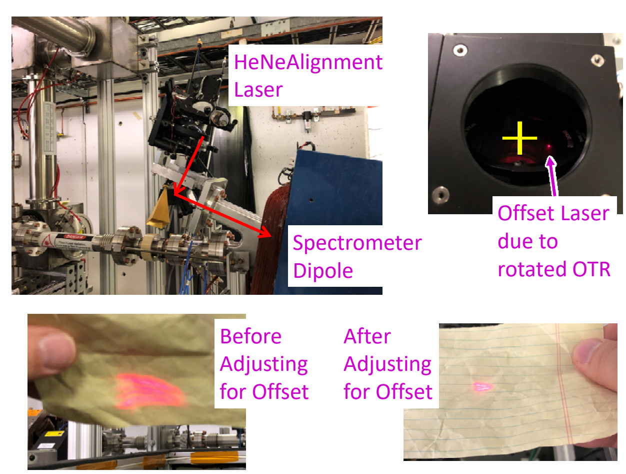


Figure 5: Alignment of the transport line is via a HeNe laser injected through a viewport before the spectrometer magnet. The before and after pictures show the distortion induced by the rotated OTR screen. The yellow cross is the ideal laser position.


Content from this work may be used under the terms of the CC BY 3.0 licence (© 2020). Any distribution of this work must maintain attribution to the author(s), title of the work, publisher, and DOI

ISBN: 978-3-95450-222-6 ISSN: 2673-5350 doi:10.18429/JACoW-IBIC2020-WEPP22

## MEASUREMENT

The measurement of the E-t phase space utilizes changes in the rf phase of the first capture cavity, CC1. The beamline was setup with the gun providing ~4.5 MeV, CC1 providing ~23 MeV, CC2 providing ~13 MeV, and 500 pC per micropulse. The beam was directed into the low energy absorber and imaged on a YAG:Ce screen with the camera system in the dispersive spectrometer line. Figure 6 shows this image of the beam focused to minimize the beta function contribution to the energy measurement.

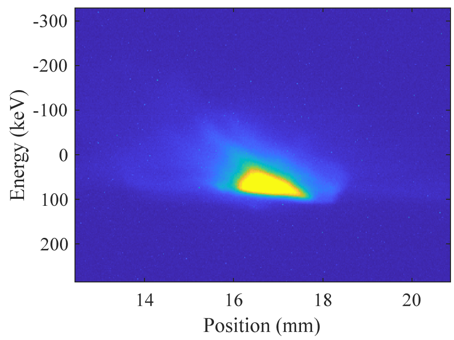


Figure 6: Beam image from the YAG:Ce screen of the spectrometer camera. The image is saturated, but the uncorrelated energy spread can be seen to be <50 KeV.

The YAG:Ce screen was then moved out, the Al-coated Si, was moved in, and the electron beam was steered as necessary to bring the light onto the streak camera. To verify that the streak camera was indeed seeing light from the electron bunches, the images from the spectrometer line were fit for the bunch length and compared to streak camera images taken in the upstream non-dispersive line.

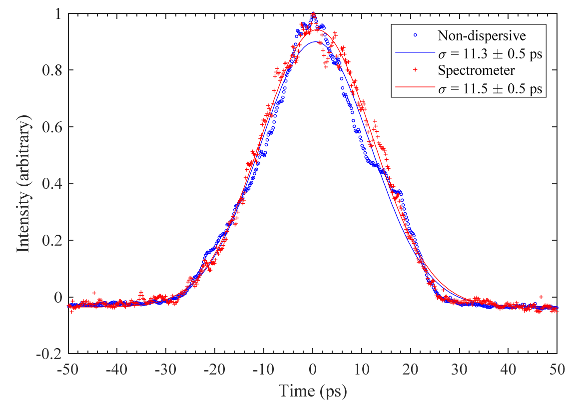


Figure 7: Projections of streak camera images from both the new spectrometer line and the upstream non-dispersive line.

The images from the spectrometer are an accumulation of 10 images, each an accumulation of 200 micropulses. The image from the non-dispersive line is 10 images of 150 micropulses. The projections of these images are fit with a gaussian plus background and shown in Fig. 7 with the fit values which are consistent.

To determine the sensitivity of the setup to changes in the E-t phase space, the phase and amplitude of CC1 were changed to move the beam off the rf crest and induce a slope in the phase space. Again, 10 images of 200 micropulses each were accumulated and summed for each of four phase values, 0, 5, 10, and 15 degrees off crest. Figure 8 shows the images from these four conditions.

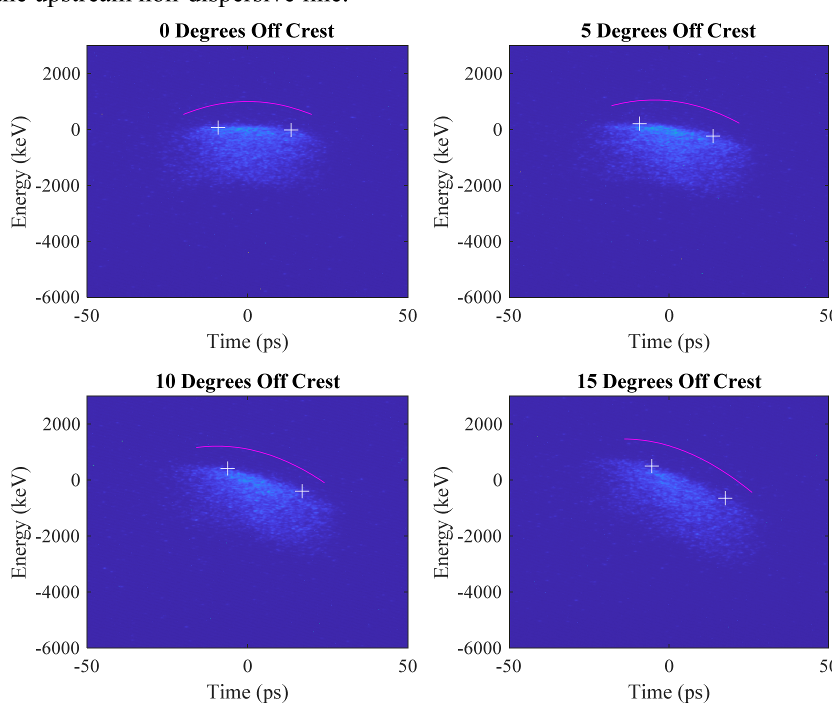


Figure 8: Streak camera images for four phase offsets of the CC1 accelerating gradient. The white crosses are the points used to determine the slope induced by the rf phase offset, and the red curves are the expected energy curve given the calibration from the points. For reference, a micropulse rms length of 11.5 ps corresponds to 6.2 degrees.

Content from this work may be used under the terms of the CC BY 3.0 licence (© 2020). Any distribution of this work must maintain attribution to the author(s), title of the work, publisher, and DOI

ISBN: 978-3-95450-222-6 ISSN: 2673-5350 doi:10.18429/JACoW-IBIC2020-WEPP22

Also shown on the images are the points (crosses) which were used to obtain the slope induced by the rf. Using those points together with the slope of the rf sinusoid we obtain a calibration constant for the 5, 10, and 15 degrees off crest cases of 10.9, 10.7, and 10.9 KeV/pixel respectively. The consistency builds confidence in the technique. Using the calibration constants, we also plot the predicted energy curvature from the sinusoidal shape of the rf from CC1 and CC2 (but not including effects from the gun).

As one can see in the images, the upper side of the image seems to fit well with the expectation, however, the vertical size does not correspond well at all with the expected energy spread, particularly the 0-degree case. From Fig. 6, we would expect something on the order of 50 to 100 KeV, but from the 0-degree image, the spread is more like 2 MeV. One possible explanation for this is poor focusing resulting from the rotated OTR screen.

An additional cross-check of the expected energy spread from the rf phase offset is seen in Fig. 9. This is the spectrometer camera image of the OTR screen for 15 degrees off crest. For a micropulse with rms length of 11.5 ps, the expected rms energy spread from the slope of the rf is ~500 KeV. Accounting for the actual sinusoidal shape of the rf results in a rms energy spread of 580 KeV. The gaussian fit in Fig. 9 has a sigma of 383 KeV. Some of this

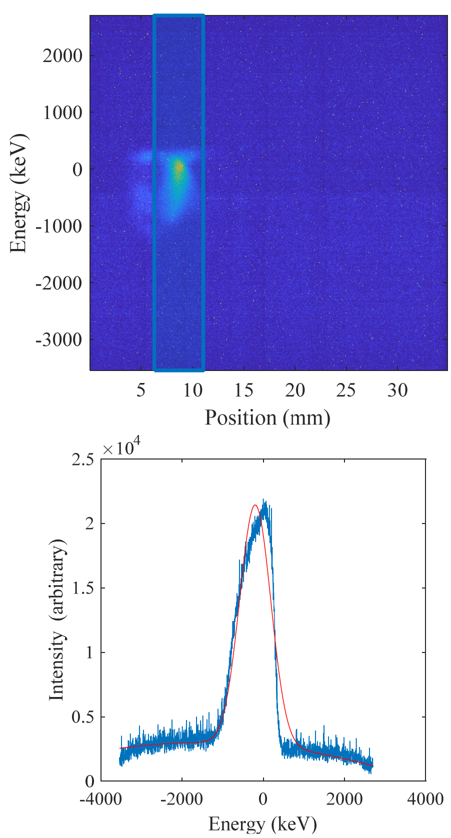


Figure 9: Top) Spectrometer camera image of beam with 15-degree rf phase offset. Bottom) The energy spread projection within the boxed region of interest and a gaussian fit with sigma of 383 KeV.

discrepancy may be due to poor positioning of the beam on the OTR screen since it appears that part of the beam may be off the screen.

## SUMMARY

At FAST, we have installed a new transport line from the OTR screen in the spectrometer beamline to the streak camera outside the enclosure. This has enabled us to make the first direct measurements of E-t phase space of electron micropulses. Preliminary results indicate that the technique should be reliable provided that the optical transport is well aligned. To that end, further improvements require a realignment of the OTR screen followed by realigning of the remaining transport.

## ACKNOWLEDGEMENTS

The authors would like to thank the FAST department staff for their efforts in support of operations at the FAST facility, and C. Drennan for support of these endeavors within the instrumentation department.

## REFERENCES

[1] P. Garbincius *et al.*, “Proposal for an accelerator R&D user facility at Fermilab’s Advanced Superconducting Test Accelerator (ASTA)”, FNAL, Batavia, IL, USA, Rep. Fermilab-TM-2568, Oct. 2013.

[2] S. Antipov *et al.*, “IOTA (Integrable Optics Test Accelerator): facility and experimental beam physics”, *J. Instrum.*, vol. 12, p. T03002, 2017. doi:10.1088/1748-0221/12/03/T03002

[3] R. Thurman-Keup, A. H. Lumpkin, and J. Thangaraj, “An optical and terahertz instrumentation system at the FAST linac at Fermilab”, in *Proc. IBIC’17*, Grand Rapids, MI, USA, Aug. 2017, pp. 342-346. doi:10.18429/JACoW-IBIC2017-WEPCC04

[4] J. Ruan *et al.*, “Commission of the drive laser system for advanced superconducting test accelerator”, in *Proc. IPAC’13*, Shanghai, China, May 2013, pp. 3061-3063, paper WEPME057.

[5] A. H. Lumpkin *et al.*, “Direct observations of submicropulse electron-beam effects from short-range wakefields in Tesla-type superconducting rf cavities”, presented at IBIC’20, Santos, Brazil, Sep. 2020, paper TUPP17, this conference.

Content from this work may be used under the terms of the CC BY 3.0 licence (© 2020). Any distribution of this work must maintain attribution to the author(s), title of the work, publisher, and DOI